Critical phenomenon in the itinerant ferromagnet $Cr_{11}Ge_{19}$ studied by scaling of the magnetic entropy change

Hui Han,[1,2] Lei Zhang,[1,*] Xiangde Zhu,[1] Haifeng Du,[1] Min Ge,[3]
Langsheng Ling,[1] Li Pi,[1,3] Changjin Zhang,[1] and Yuheng Zhang[1,3]

[1]*High Magnetic Field Laboratory, Chinese Academy of Sciences, Hefei 230031, China*

[2]*University of Science and Technology of China, Hefei 230026, China*

[3]*Hefei National Laboratory for Physical Sciences at the Microscale, University of Science and Technology of China, Hefei 230026, China*

(Dated: September 12, 2016)

Abstract

Critical phenomenon of the noncentrosymmetric $Cr_{11}Ge_{19}$, which exhibits an itinerant ferromagnetic ground state, is investigated by scaling of the magnetic entropy change [$\Delta S_M(T,H)$]. It is found that parameters δ_{FWHM} (the full width at half maximum), $-\Delta S_M^{max}$ (the maximum of the magnetic entropy change), and RCP (the relative cooling power) of $\Delta S_M(T)$ are governed by the power law of critical exponents. With the critical exponents, $\Delta S_M(T,H)$ curves are scaled into a universal curve independent of temperature and field, which suggests that the magnetic transition is of a second order type. The universal collapse of $\Delta S_M(T,H)$ indicates that the critical behavior of $Cr_{11}Ge_{19}$ can be well described by the scaling laws for the critical phenomenon. Moreover, the ΔS_M follows the power law of H^n with $n(T,H) = dln|\Delta S_M|/dln(H)$. The temperature dependence of n values reach minimum at $\sim$ 71.5 K. Based on the magnetic specific change $\Delta C_p(T,H)$, the actual magnetic transition temperature is strictly determined as $T_C = 71.3 \pm 0.2$ K for the single crystal $Cr_{11}Ge_{19}$.

PACS numbers: 75.30.Sg, 75.40.-s, 75.40.Cx

Keywords: magnetic entropy change; critical phenomenon; itinerant ferromagnetism; single crystal; scaling

*Corresponding author. Email: zhanglei@hmfl.ac.cn

I. INTRODUCTION

Chiral magnetic material has triggered great interests recently due to the discovery of exotic non-collinear magnetic configurations, such as skyrmion, magnetic soliton, and chiral bobber [1–4]. These findings pave a distinctive way to the application in spintronics [5, 6]. These attractive magnetic configurations usually emerge in noncentrosymmetric helimagnetic compounds, such as MnSi, FeGe, $Fe_{1-x}Co_xSi$, and Cu_2OSeO_3 [7–10]. In a noncentrosymmetric structure, the lack of inversion symmetry usually results in the Dzyaloshinsky-Moriya (DM) interaction, which is 1∼2 orders of magnitude smaller than the ferromagnetic coupling. The competition between the DM interaction and the ferromagnetic coupling causes the formation of the helimagnetic ground sate as well as the conical magnetic ordering in moderate magnetic fields [11]. Generally, non-collinear spin textures emerge just below the magnetic transition temperature in narrow ranges of field (H) and temperature (T) [12–15]. Therefore, the investigation of non-collinear magnetic configurations is of great importance not only for application but also for fundamental physics [3].

Due to the noncentrosymmetric and chiral structure, $Cr_{11}Ge_{19}$ is a candidate material in which a non-collinear magnetic configuration is expected [16]. The cell of $Cr_{11}Ge_{19}$, which belongs to tetragonal symmetry with space group $P\overline{4}n2$, is crystallized as Nowotny chimney ladders (NCLs) [17]. A chiral structure of Cr-Cr bonds can be found along the c-axis. Recent investigations have demonstrated that $Cr_{11}Ge_{19}$ displays a complex itinerant ferromagnetic ground state [18–21]. However, the magnetic behavior of $Cr_{11}Ge_{19}$ does not obey the Stoner model which is a conventional theory describing an itinerant ferromagnet [22]. Our previous study has suggested that the ferromagnetic ground state of $Cr_{11}Ge_{19}$ is formed by polarized magnetic moments along the c-axis, while the long-range magnetic coupling is established within the ab plane [23]. Meanwhile, for an itinerant ferromagnet with DM interaction, a quantum critical behavior may emerge when the helimagnetism is suppressed, such as non-Fermi-liquid behavior and unusual magnetic excitation [24–28]. Thus, the investigation of $Cr_{11}Ge_{19}$ is of great importance for understanding the magnetic interactions in noncentrosymmetric ferromagnets.

As we know, the magnetic entropy changes when the magnetic transition occurs, which provides an effective means to study the magnetic transition [29]. In this work, we investigate the critical phenomenon of the itinerant ferromagnetic $Cr_{11}Ge_{19}$ single crystal by scaling of

the magnetic entropy change $[\Delta S_M(T,H)]$. With the critical exponents, the $\Delta S_M(T,H)$ curves are well scaled into a universal curve independent of temperature and field. Moreover, the actual magnetic transition temperature is strictly determined from the temperature dependence of n values and the magnetic specific change $\Delta C_p(T,H)$.

II. EXPERIMENT

A single crystal $Cr_{11}Ge_{19}$ was synthesized by a chemical vapor transport (CVT) method as described by R. Neddermann *et al* [30]. The pieces of chromium and germanium in mol ratio of $45:55$ and about 50 mg iodine were put in an evacuated quartz tube. The tube was then placed in a two zone furnace and heated to 1053 K. After keeping for 4 days, the source end was kept at 1053 K and growth zone was raised to 1153 K. After 10 days growth, single crystals in millimeter size can be obtained. The chemical composition and phase purity were carefully checked elsewhere [23]. The measurement of magnetization was performed using a Quantum Design Vibrating Sample Magnetometer (SQUID-VSM). In order to ensure each curve was initially magnetized, the sample was firstly heated adequately above the phase transition temperature for ten minutes. Then, the measurement of the isothermal magnetization was carried out after cooling to the target temperature under zero magnetic field. The magnetic field was relaxed for two minutes before data collection.

III. RESULTS AND DISCUSSION

Figure 1 (a) shows the temperature dependence of magnetization $[M(T)]$ for single crystal $Cr_{11}Ge_{19}$ with the magnetic field $H//c$ and $H//b$ respectively. The lattice structure of $Cr_{11}Ge_{19}$ is crystallized as NCLs, as depicted in the inset of Fig. 1 (a). The cell belongs to tetragonal symmetry with equal a and b axes. A prominent paramagnetic-ferromagnetic transition occurs to the $M(T)$ curves when $H//c$. However, this magnetic transition becomes weak when $H//b$, indicating that easy orientation of magnetization is along the c-axis. The magnetic transition temperature $T_C \sim 72$ K is approximately determined from the sharpest point on $M(T)$ curve with $H//c$. Generally, T_C can be roughly determined from the peak on dM/dT. Figure 1 (b) shows the $M(T)$ curves under different fields with $H//c$, and the upper-left inset gives dM/dT vs. T. T_C determined from the minimum from $dM/dT(T)$

curves is plotted in the bottom-right inset of Fig. 1 (b), which shows that T_C determined by this method increases monotonously with the increase of H. It obtained that T_C is $\sim$ 86 K when H = 10 kOe, which is close to that reported by N. J. Ghimire, *et al*. from the polycrystalline sample [22]. Figure 1 (c) shows the initial isothermal magnetization $[M(H)]$ around T_C with $H//c$. The inset of Fig. 1 (c) gives the $M(H)$ curves with $H//a$, $H//b$, $H//c$ at 5 K, which confirms that the easy orientation of magnetization is along the c-axis and that a and b-axis are equivalent in magnetism. According to the Stoner theory which is a conventional model describing the itinerant ferromagnet, the magnetic behavior should be follow [31]:

$$M^2 = -\frac{A}{B} + \frac{1}{B}\left(\frac{H}{M}\right) \tag{1}$$

where A and B are parameters independent of H. Equation (1) means that the Arrott plot of H/M vs. M^2 should be a series of straight lines. However, it has been demonstrated that $Cr_{11}Ge_{19}$ does not obey the conventional Arrott plot [22]. Therefore, a modified Arrott plot of $H/M^{1/\gamma}$ vs. $M^{1/\beta}$ (β and γ are critical exponents) is performed, as plotted in Fig. 1 (d). It gives that $\beta = 0.345(4)$ and $\gamma = 1.318(2)$. The modified Arrott plot of $H/M^{1/\gamma}$ vs. $M^{1/\beta}$ exhibit straight lines in high field region, and the line at T_C goes through the origin. The intercept on the $H/M^{1/\gamma}$ coordinate axis is plotted in the inset of Fig. 1 (d), which shows that $T_C \sim 72$ K.

Based on the thermodynamical theory, the magnetic entropy change $[\Delta S_M(T,H)]$ induced by the external field is given by: [32]:

$$\Delta S_M(T,H) = \int_0^{H^{max}} \left[\frac{\partial S(T,H)}{\partial H}\right]_T dH \tag{2}$$

with Maxwell's relation: $[\partial S(T,H)/\partial H]_T$=$[\partial M(T,H)/\partial T]_H$ [33], $\Delta S_M(T,H)$ is written as:

$$\Delta S_M(T,H) = S_M(T,H) - S_M(T,0) = \int_0^{H^{max}} \left[\frac{\partial M(T,H)}{\partial T}\right]_H dH \tag{3}$$

where H is the external magnetic field, T is the temperature, and H^{max} is the maximum of external magnetic field. Based on the initial $M(H)$ curves in Fig. 1 (c), the temperature dependence of ΔS_M $[-\Delta S_M(T)]$ curves under different H are calculated, which are plotted in Fig. 2 (a). For each $-\Delta S_M(T)$ curve, a maximum value appears around $T_C \sim 72$ K, and the value of $-\Delta S_M(T)$ almost decreases symmetrically on both sides.

The magnitude of $-\Delta S_M(T)$ raises with the increase of H, and reaches a maximum value of 1.22 J.kg^{-1}K^{-1} when H = 7 T. Meanwhile, the $-\Delta S_M(T)$ curve broadens with

the increase of H. Figure 2 (b), (c), and (d) plot parameters for δ_{FWHM} (the full width at half maximum), $-\Delta S_M^{max}$ (the maximum of the magnetic entropy change), and RCP (the relative cooling power) as a function of H. Generally, $-\Delta S_M^{max}$ obeys the power law of H as [34, 35]:

$$-\Delta S_M^{max} \propto H^n \tag{4}$$

where n depends on the magnetic state of the sample. Fitting of the $-\Delta S_M^{max}(H)$ gives that $n = 0.596(6)$, as shown in Fig. 2 (b). Theoretically, there is $n = 1+(\beta-1)/(\beta+\gamma)$ when $T = T_C$ (where β, γ and δ are the critical exponents) [34]. For $Cr_{11}Ge_{19}$ with $\beta = 0.345(4)$, $\gamma = 1.318(2)$ and $\delta = 4.821(2)$ [23], it can be calculated that $n = 0.606(7)$. The value obtained by the experiment agrees well with that deduced from the critical analysis. Moreover, δT_{FWHM} is also governed by the power law, as given in Fig. 2 (c). The fitting of $\delta T_{FWHM}(H)$ gives that $\delta T_{FWHM} \propto H^{0.566(1)}$. Generally, $RCP(S)$ is an important parameter for the magnetic entropy change, which is defined as [36]:

$$RCP(S) = -\Delta S_M^{max} \times \delta T_{FWHM} \tag{5}$$

In fact, $RCP(S)$ has the relation with H as $RCP(S) = mH^c$ with $c = 1+1/\delta$ [37]. Experimentally, it is obtained that $c = 1.167(4)$. Based on the critical analysis, it gives that $c = 1.207(4)$, which approximates to the experimental result.

Based on the scaling relation of the critical phenomenon, a universal scaling of $\Delta S_M(T,H)$ has been proposed [34, 35, 37]. For a second-order magnetic transition, it is suggested that $\Delta S_M(T,H)$ should collapse into a universal curve, which is independent of external magnetic field and temperature. However, for a first-order one, the scaling of $\Delta S_M(T,H)$ should exhibit a dispersive behavior. The $\Delta S_M(T,H)$ is normalized by $|\Delta S_M/\Delta S_M^{max}|$, and the temperature is normalized by reference temperature T_r into re-scaled temperature θ. After normalizing the curves, T_{r1} and T_{r2} are just corresponding to $\theta = -1$ and $\theta = +1$ respectively. The re-scaled temperature θ is defined as [37]:

$$\theta = \begin{cases} \theta_- = (T_C - T)/(T_{r1} - T_C), T \leq T_C \\ \theta_+ = (T - T_C)/(T_{r2} - T_C), T > T_C \end{cases} \tag{6}$$

where T_{r1} and T_{r2} are the reference temperatures below and above T_C respectively, which corresponds to $\Delta S_M(T_{r1}, T_{r2}) = \frac{1}{2}\Delta S_M^{max}$. The construction of a universal scaling of the experimental $\Delta S_M(T,H)$ are plotted in Fig. 3 (a). The ΔS_M is normalized as $\Delta S_M/\Delta S_M^{max}$,

and the temperature is plotted as θ. All experimental data collapse into a single universal curve. The good convergence of the $\Delta S_M(T,H)$ curves indicates the magnetic transition is of the second-order type. As one can see, this universal curve is independent of the external measurement conditions, which is just determined by the intrinsic magnetization. The inset of Fig. 3 (a) gives the field dependence of T_{r1} and T_{r2}, which shows that both T_{r1} and T_{r2} are field dependent.

For the critical phenomenon in a second order magnetic transition, the $\Delta S_M(T,H)$ curves can also be scaled with the critical exponents. According to the scaled equation of state $[\frac{H}{M^\delta} = f(\frac{\varepsilon}{M^{1/\beta}})]$, Eq. (1) can be rewritten into another form [38, 39]:

$$\Delta S_M(T,H) = H^{\frac{(1-\alpha)}{\Delta}} g\left(\frac{\varepsilon}{H^{\frac{1}{\Delta}}}\right) \tag{7}$$

where α, β, γ, δ, Δ are the critical exponents, and $\varepsilon = (T - T_C)/T_C$ is the reduced temperature. There is relation:

$$\begin{cases} \alpha = 2 - 2\beta - \gamma \\ \Delta = \delta \times \beta \end{cases} \tag{8}$$

Figure 3 (b) plots $\frac{\Delta S_M}{H^{(1-\alpha)/\Delta}}$ vs. $\frac{\varepsilon}{H^{1/\Delta}}$. One can see all data for different magnetic fields and temperatures collapse into a universal curve. These $\Delta S_M(T)$ curves under different H exactly overlap with each other, which suggests that the critical behavior of $Cr_{11}Ge_{19}$ can be well described by the scaling laws for the critical phenomenon.

For a second order phase transition, ΔS_M follows the power law of $\Delta S_M \propto H^n$ [34]. Therefore, the value n can be calculated as:

$$n(T,H) = \frac{d\ln(|\Delta S_M(T,H)|)}{d\ln(H)} \tag{9}$$

Figure 4 (a) shows the field dependence of $-\Delta S_M$ at different temperatures. As can be seen, all isothermal entropy changes increase monotonically with the applied magnetic field for $Cr_{11}Ge_{19}$. Based on Fig. 4 (a), the temperature dependence of n under different H are calculated and shown in Fig. 4 (b). The n value reaches ~ 0.8 far below T_C, and approaches $\sim$1.8 far above T_C. The minimum of $n(T)$ for different H locates at T_C. It is obtained that the minimum value of n is 0.58 at $T_C \sim 71.5$ K, which is in agreement with that obtained from fitting of $-\Delta S_M^{max}(H)$ plotted in Fig. 2 (b). The $n(T)$ curves can be also well scaled by θ, as shown in the inset of Fig. 4 (b). All values of n and the tendency match the universal law for n change [40, 41].

Generally, the magnetic phase transition T_C can be roughly determined by the peak on $dM(T)/dT$ vs. T curve. However, in reality the external magnetic field has an effect on the peak, as shown in Fig. 1 (b). Thus, T_C determined by this method is affected by the external field. The actual T_C is hard to be obtained strictly because the external magnetic field will affect the magnetic measurement. More strictly, the magnetic transition temperature can be actually obtained from the magnetic specific heat change (ΔC_P). The $\Delta C_P(T,H)$ can be obtained from the change of $\Delta S_M(T,H)$ as [42]:

$$\Delta C_p(T,H) = C_p(T,H) - C_p(T,0) = T\frac{\partial \Delta S_M(T,H)}{\partial T} \tag{10}$$

The temperature dependence of $-\Delta C_P$ under different H is depicted in Fig. 5. Obviously, there is $-\Delta C_P < 0$ for $T < T_C$ and $-\Delta C_P > 0$ for $T > T_C$. The $-\Delta C_P(T)$ curve changes sharply from negative to positive value at T_C, corresponding to the change from ferromagnetic phase to paramagnetic region. It can be seen that all $-\Delta C_P(T)$ curves change sharply almost at a same temperature point, regardless of different external fields. This phenomenon is also valid in other materials [41, 42]. The actual magnetic transition temperature can be determined by temperature corresponding to the zero point of ΔC_P $[\Delta C_P(T,H)|_{T=T_C} = 0]$. Subsequently, it is obtained that the actual magnetic transition temperature $T_C = 71.3 \pm 0.2$ K for the single crystal $Cr_{11}Ge_{19}$. The T_C obtained from $\Delta C_P(T,H)$ is slight smaller than that determined from the $M(T)$ curve, indicating that T_C is slightly increased by the external magnetic field.

IV. CONCLUSION

In summary, the critical phenomenon of noncentrosymmetric $Cr_{11}Ge_{19}$ single crystal is studied by scaling of $\Delta S_M(T,H)$. The parameters of $\Delta S_M(T,H)$ (δ_{FWHM}, $-\Delta S_M^{max}$, and RCP) are governed by the power law of critical exponents. The $\Delta S_M(T,H)$ curves are well scaled into a universal curve independent of T and H. The universal collapse of $\Delta S_M(T,H)$ curves indicates that the magnetic transition is of a second order type and the critical behavior of $Cr_{11}Ge_{19}$ can be well described by the scaling laws for the critical phenomenon. The ΔS_M follows the power law of H^n with $n(T,H) = dln|\Delta S_M|/dln(H)$. The temperature dependence of n values reach the minimum at ~ 71.5 K. Based on the magnetic specific change $\Delta C_P(T,H)$, it is strictly obtained that the actual magnetic transition temperature

$T_C = 71.3 \pm 0.2$ K for the single crystal $Cr_{11}Ge_{19}$.

V. ACKNOWLEDGEMENTS

This work was supported by the State Key Project of Fundamental Research of China through Grant No. 2011CBA00111, the National Natural Science Foundation of China (Grant Nos. 11574322, U1332140, 11474289, U1532267, and 11474290), the Foundation for Users with Potential of Hefei Science Center (CAS) through Grant No. 2015HSC-UP001.

---

[1] X. Yu, Y. Onose, N. Kanazawa, J. Park, J. Han, Y. Matsui, N. Nagaosa, Y. Tokura, Nature (London) **465** (2010) 901.

[2] Y. Togawa, T. Koyama, K. Takayanagi, S. Mori, Y. Kousaka, J. Akimitsu, S. Nishihara, K. Inoue, A. S. Ovchinnikov, J. Kishine, Phys. Rev. Lett. **108** (2012) 107202.

[3] F. N. Rybakov, A. B. Borisov, S. Blugel, N. S. Kiselev, Phys. Rev. Lett. **115** (2015) 117201.

[4] S. Muuhlbauer, B. Binz, F. Jonietz, C. Pfleiderer, A. Rosch, A. Neubauer, R. Georgii, P. Boni, Science **323** (2009) 915.

[5] A. Fert, V. Cros, J. Sampaio, Nat. Nanotechnol. **8** (2013) 152.

[6] X. Z. Yu, N. Kanazaw, Y. Onose, K. Kimoto, W. Z. Zhang, S. Ishiwata, Y. Matsui, Y. Tokura, Nat. Mater. **10** (2011) 106.

[7] F. Jonietz, S. Muhlbauer, C. Pfleiderer, A. Neubauer, W. Munzer, A. Bauer, T. Adams, R. Georgii, P. Boni, R. A. Duine, K. Everschor, M. Garst, A. Rosch, Science **330** (2010) 1648.

[8] K. Shibata, J. Iwasaki, N. Kanazawa, S. Aizawa, T. Tanigaki, M. Shirai, T. Nakajima, M. Kubota, M. Kawasaki, H. S. Park, D. Shindo, N. Nagaosa, Y. Tokura, Nat. Naonotechol. **10** (2015) 589.

[9] P. Milde, D. Kohler, J. Seidel, L. M. Eng, A. Bauer, A. Chacon, J. Kindervater, S. Muhlbauer, C. Pfleiderer, S. Buhrandt, C. Schutte, A. Rosch, Science **340** (2013) 1076.

[10] T. Adams, A. Chacon, M. Wagner, A. Bauer, G. Brandl, B. Pedersen, H. Berger, P. Lemmens, C. Pfleiderer, Phys. Rev. Lett. **108** (2012) 237204.

[11] P. Bak and M. H. Jensen, J. Phys. C: Solid State Phys. **13** (1980) L881.

[12] U. K. Roβler, A. N. Bogdanov, C. Pfleiderer, Nature (London) **442** (2006) 797.

[13] A. Bauer and C. Pfleiderer, Phys. Rev. B **85** (2012) 214418.

[14] A. Bauer, M. Garst, C. Pfleiderer, Phys. Rev. B **93** (2016) 235144.

[15] K. Tsuruta, M. Mito, H. Deguchi, J. Kishine, Y. Kousaka, J. Akimitsu, K. Inoue, Phys. Rev. B **93** (2016) 104402.

[16] M. N. Wilson, A. B. Butenko, A. N. Bogdanov, T. L. Monchesky, Phys. Rev. B **89** (2014) 094411.

[17] T. Caillat, J. P. Fleurial, A. Borshchevsky, J. Alloys Compd. **252** (1997) 12.

[18] H. Vollenkle, A. Preisinger, H. Nowotny, A. Wittmann, Z. Kristallogr. **124** (1967) 9.

[19] V. L. Zagryazhskii, P. V. Geld, A. K. Shtolts, Sov. Phys. J. **11** (1968) 23.

[20] M. Kolenda, J. Stoch, A. Szytula, J. Magn. Magn. Mater. **20** (1980) 99.

[21] P. Pecheur, G. Toussaint, H. Kenzari, B. Malaman, R. Welter, J. Alloys Compd. **262-263** (1997) 363.

[22] N. J. Ghimire, M. A. McGuire, D. S. Parker, B. C. Sales, J. Q. Yan, V. Keppens, M. Koehler, R. M. Latture, D. Mandrus, Phys. Rev. B **85** (2012) 224405.

[23] H. Han, L. Zhang, X. D. Zhu, H. F. Du, M. Ge, L. S. Ling, L. Pi, C. J. Zhang, Y. H. Zhang, Anisotropic magnetic coupling with a two-dimensional characteristic in noncentrosymmetric $Cr_{11}Ge_{19}$, where critical exponents $\beta = 0.345(4)$, $\gamma^{cal} = 1.318(2)$, and $\delta = 4.821(2)$ are obtained, to be pulished.

[24] N. Manyala, Y. Sidis, J. F. DiTusa, G. Aeppli, D. P. Young, Z. Fisk, Nature (London) **404** (2000) 581.

[25] C. Pfleiderer, S. R. Julian, G. G. Lonzarich, Nature (London) **414** (2001) 427.

[26] H. Watanabe, S. A. Parameswaran, S. Raghu, A. Vishwanath, Phys. Rev. B **90** (2014) 045145.

[27] C. Pfleiderer, G. J. McMullan, S. R. Julian, G. G. Lonzarich, Phys. Rev. B **55** (1997) 8330.

[28] D. A. Sokolov, M. C. Aronson, W. Gannon, Z. Fisk, Phys. Rev. Lett. **96** (2006) 116404.

[29] M. Ge, L. Zhang, D. Menzel, H. Han, C. Jin, C. Zhang, L. Pi, S. Tan, Y. Zhang, J. Alloys Compd. **649** (2015) 46.

[30] R. Neddermann, R. Wartchow, M. Binnewies, Z. anorg. allg. Chem. **624** (1998) 733.

[31] D. M. Edwards and E. P. Wohlfarth, Proc. Roy. Soc. A **303,** 127 (1968).

[32] V. Pecharsky, K. Gscheidner, J. Magn. Magn. Mater. **200** (1999) 44.

[33] D. J. Griffiths, *Introduction to electrodynamics (Third ed.)*. Prentice Hall. pp. 559-562. (1999).

[34] V. Franco, J. S. Blazquez, A. Conde, Appl. Phys. Lett. **89** (2006) 222512.

[35] V. Franco, A. Conde, J. M. Romero-Enrique, J. S. Blazquez, J. Phys.: Condens. Matter **20** (2008) 285207.

[36] J. Y. Fan, B. Hong, D. Lu, Y. G. Shi, L. S. Ling, L. Zhang, W. Tong, L. Pi, Y. H. Zhang, Physica B **405** (2010) 3120.

[37] V. Franco, A. Conde, Int. J. Refrigerat. **33** (2010) 465.

[38] B. Widom, J. Chem. Phys. **43** (1965) 3898.

[39] R. B. Griffiths, Phys. Rev. Lett. **423** (1969) 17.

[40] R. Caballero-Flores, N. S. Bingham, M. H. Phan, M. A. Torija, C. Leighton, V. Franco, A. Conde, T. L. Phan, S.C. Yu, and H. Srikanth, J. Phys.: Condens. Matter **26** (2014) 286001.

[41] R. Mnassri, N. Chniba-Boudjada, A. Cheikhrouhou, J. Alloys Compd. **640** (2015) 183.

[42] X. X. Zhang, G. H. Wen, F. W. Wang, W. H. Wang, C. H. Yu, G. H. Wu, Appl. Phys. Lett. **77** (2000) 3072.

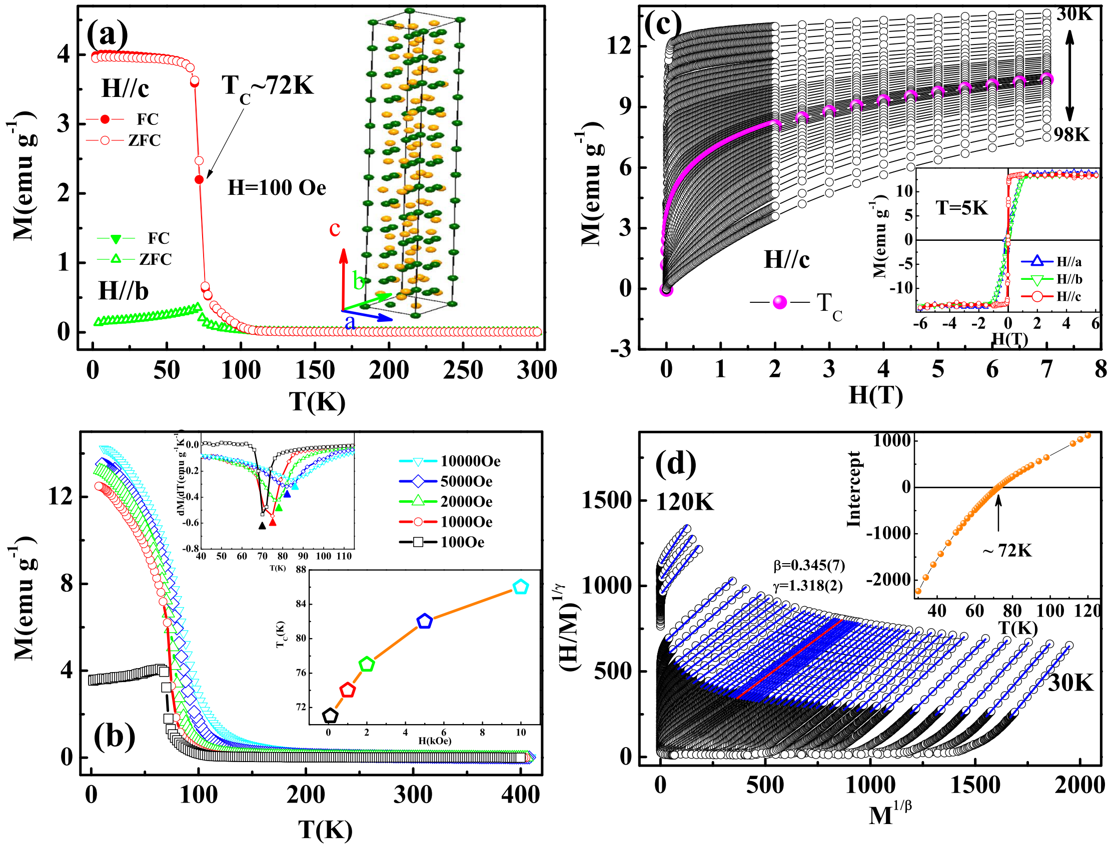

FIG. 1: (Color online) (a) Temperature dependence of magnetization $[M(T)]$ for $Cr_{11}Ge_{19}$ with $H//c$ and $H//b$ axes (the inset depicts the crystal structure); (b) $M(T)$ along the c-axis under different H (the upper-left inset gives the dM/dT vs. T, and the bottom-right plots T_C vs. H); (c) the initial isothermal magnetization $[M(H)]$ around T_C (the inset gives $M(H)$ at 5 K with $H//a$, $H//b$, and $H//c$ respectively); (d) the modified Arrott plot of $H/M^{1\gamma}$ vs. $M^{1/\beta}$ (the inset gives the intercept as a function of temperature).

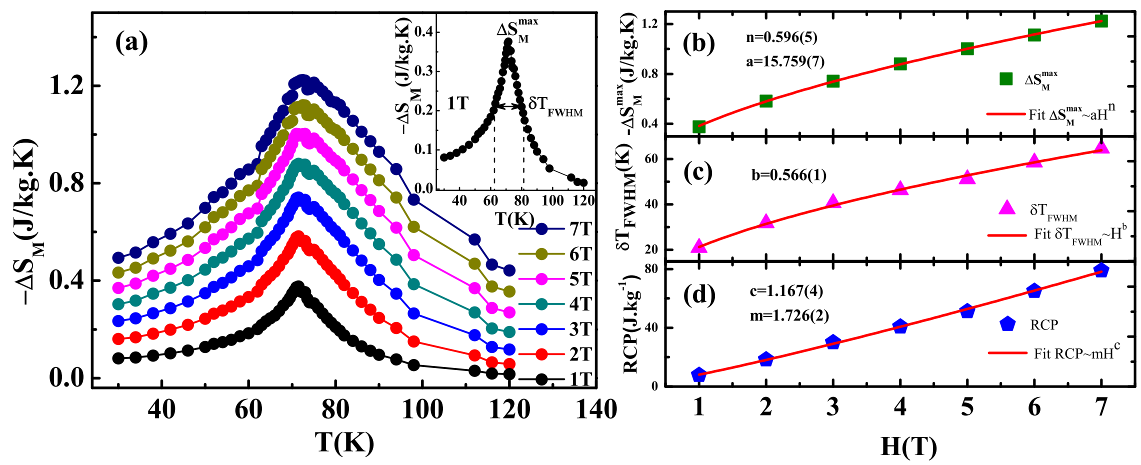

FIG. 2: (Color online) (a) Temperature dependence of ΔS_M $[-\Delta S_M(T)]$ under different H (the inset plot $-\Delta S_M(T)$ for $H = 1$ T); the parameters for (b) $-\Delta S_M^{max}$, (c) δ_{FWHM}, and (d) RCP as a function of H (solid curves are fitted).

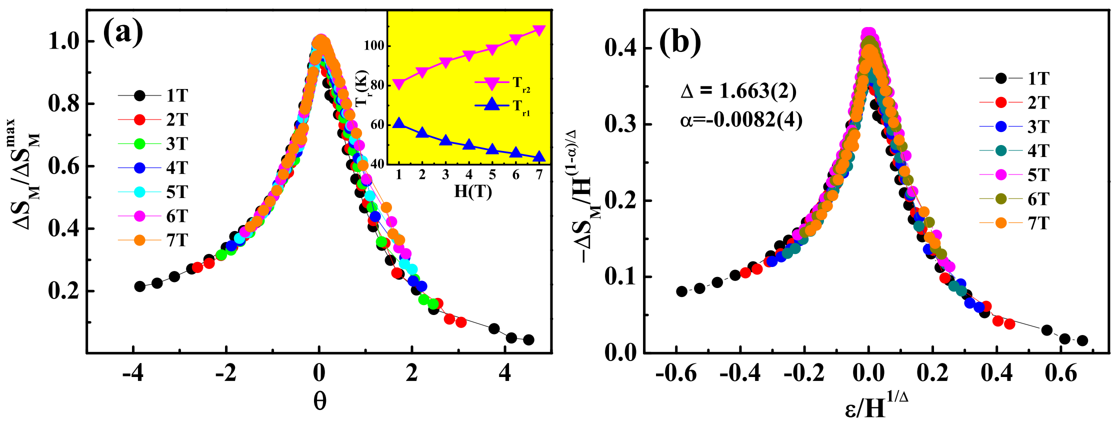

FIG. 3: (Color online) Scaling of the $\Delta S_M(T, H)$ curves: (a) the normalized $\Delta S_M(T, H)$ as a function of θ (the inset gives T_{r1} and T_{r2} as a function of H); (b) scaled $\Delta S_M(T, H)$ vs. scaled temperature using critical exponents.

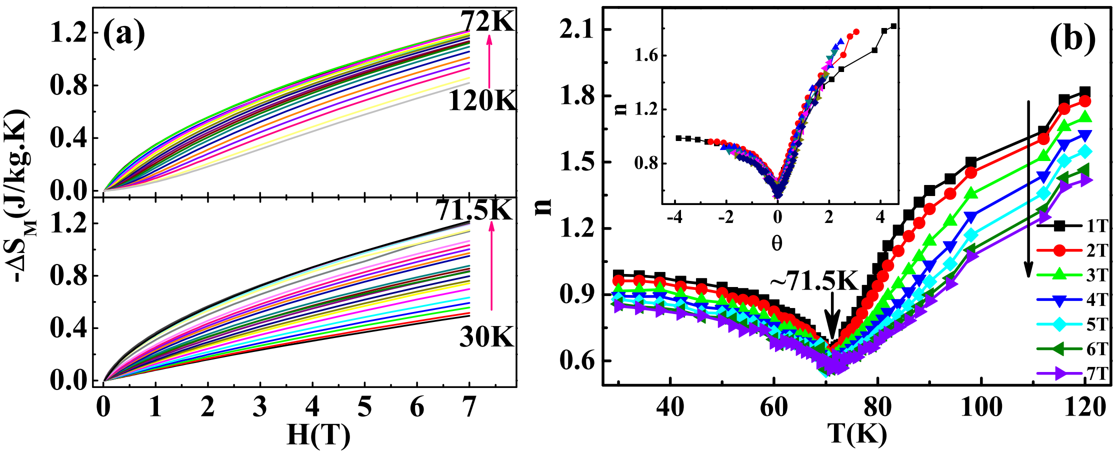

FIG. 4: (Color online) (a) Field dependent of $-\Delta S_M$ for different temperatures; (b) the temperature dependence of n under different H (the inset gives n vs. θ).

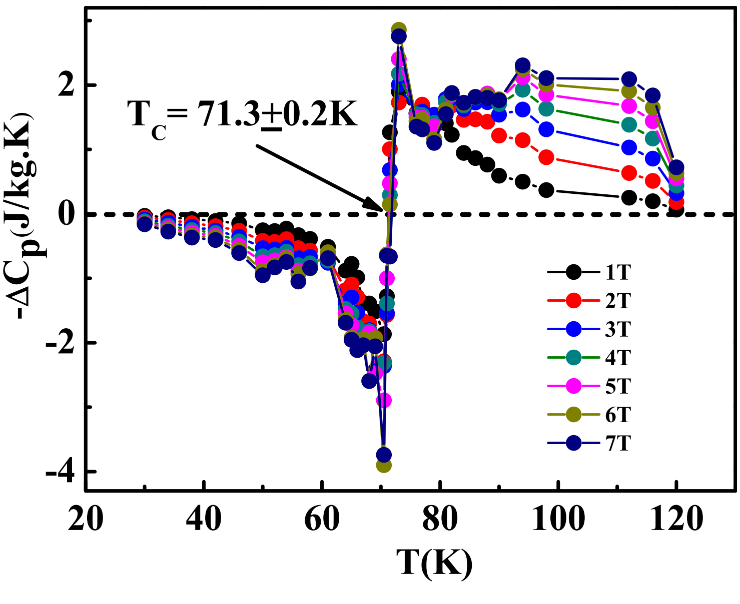

FIG. 5: (Color online) Temperature dependence of $-\Delta C_p$ under different H.